Mouse VAP33 is associated with the endoplasmic reticulum and microtubules

P. A. Skehel*†, R. Fabian-Fine‡, and E. R. Kandel§

*Division of Neurophysiology, National Institute for Medical Research, The Ridgeway, Mill Hill, London, NW7 1AA, United Kingdom; ‡Department of Biological Sciences, The Open University, Milton Keynes, MK7 6AA United Kingdom; and §Center for Neurobiology and Behavior, Howard Hughes Medical Institute, Columbia University, New York, NY 10032

Contributed by E. R. Kandel, November 9, 1999

VAMP/synaptobrevin is a synaptic vesicle protein that is essential for neurotransmitter release. Intracellular injection of antisera against the *Aplysia californica* VAMP/synaptobrevin-binding protein ApVAP33 inhibited evoked excitatory postsynaptic potentials (EPSPs) in cultured cells, suggesting that this association may regulate the function of VAMP/synaptobrevin. We have identified and characterized a mouse homologue of ApVAP33, mVAP33. The overall domain structure of the proteins is conserved, and they have similar biochemical properties. mVAP33 mRNA is detectable in all mouse tissues examined, in contrast to the more restricted expression seen in *A. californica.* We analyzed the cellular distribution of mVAP33 protein in brain slices and cultured cortical cells by light and electron microscopy. Although present at higher levels in neurons, immunoreactivity was detected throughout both neurons and glia in a reticular pattern similar to that of endoplasmic reticulum-resident proteins. mVAP33 does not colocalize with VAMP/synaptobrevin at synaptic structures, but expression overlaps with lower levels of VAMP/synaptobrevin in the soma. Ultrastructural analysis revealed mVAP33 associated with microtubules and intracellular vesicles of heterogeneous size. In primary neuronal cultures, large aggregates of mVAP33 are also detected in short filamentous structures, which are occasionally associated with intracellular membranes. There is no evidence for accumulation of mVAP33 on synaptic vesicles or at the plasma membrane. These data suggest that mVAP33 is an endoplasmic-reticulum–resident protein that associates with components of the cytoskeleton. Any functional interaction between mVAP33 and VAMP/synaptobrevin, therefore, most likely involves the delivery of components to synaptic terminals rather than a direct participation in synaptic vesicle exocytosis.

Eukaryotic cells contain elaborate and dynamic systems of membrane-bound organelles and transport vesicles. The trafficking and integrity of these structures rely on a complex series of protein–protein and protein–lipid interactions that are generally conserved in all eukaryotes (1–3). Neurons contain specialized organelles, the synaptic vesicles, that facilitate the sustained, rapid, and coordinated release of neurotransmitter into the synaptic cleft (4, 5). The SNAP receptor (SNARE) hypothesis was developed to describe the mechanism whereby a vesicle interacts with and subsequently fuses with a target membrane (6, 7). As originally proposed, proteins on the vesicle membrane, or v-SNAREs, combine with proteins on the target membrane, or t-SNAREs, to generate a receptor complex for the ATPase NSF and α-SNAP. The complex dissociates after ATP hydrolysis. The exact relationship between these biochemical events and membrane fusion is still a matter of debate (8, 9). Although originally described in relation to the interaction of synaptic vesicles with the presynaptic plasmallema, a number of v- and t-SNARE proteins have been identified for several intracellular trafficking events (3). A characterizing feature of the complex formed between v- and t-SNAREs is its stability in detergent. Recently, the crystal structure of a soluble form of the complex formed between the v-SNARE synaptobrevin and the t-SNAREs syntaxin and SNAP-25 was solved, revealing a long four-helix coiled-coil as the basis of this stability. Synaptobrevin and the t-SNAREs syntaxin and SNAP-25 accumulate on different membranes, and a number of additional proteins have been identified that are capable of interacting with synaptobrevin, syntaxin, and SNAP-25 (10–19). These interactions may function to regulate the formation of the SNARE complex or the intracellular targeting of its constituents. Alternatively, such interactions may be part of regulatory or biosynthetic mechanisms quite distinct from vesicle exocytosis.

ApVAP33 (*Aplysia* VAMP/synaptobrevin-associated protein of 33 kDa) was originally identified by its ability to interact with VAMP/synaptobrevin in a yeast two-hybrid assay (18). In *Aplysia* sensory-motorneuron cocultures, it was shown that presynaptic injection of ApVAP33-specific antisera inhibited postsynaptically measured excitatory postsynaptic potentials (EPSPs) suggesting that an interaction between ApVAP33 and VAMP/synaptobrevin was required for efficient synaptic transmission in this culture. Homologous genes have been identified in humans, rats, and *Saccharomyces cerevisiae* (20–22). To analyze the function of the protein in a more genetically amenable vertebrate context, we have characterized a mouse homologue of ApVAP33.

Experimental Procedures

Cloning of Mouse VAP33. The similarity between ApVAP33 and a human expressed sequence tag was used to design two degenerate oligonucleotides for a PCR generating a DNA fragment of about 210 bp from mouse brain cDNA: 5′-GAGTTAAGATTCAA(GATC)GG(GATC)CC(GATC)TTCA-3′ and 5′-CTTGTTCTTTTCATTCGGATCATA-3′. This DNA was then used as a probe to screen a plasmid-based mouse brain cDNA library by hybridization (CLONTECH).

RNA Isolation and Northern Blot Hybridization Analysis. Samples of the indicated tissues were dissected from adult male C57BL6 mice. Total RNA was then purified by using the TRIzol Reagent (GIBCO/BRL) as directed by the manufacturer. RNA (10 μg) from each tissue was denatured and separated on a 1% agarose/4-morpholinepropanesulfonic acid gel, transferred to Hybond N+ (Amersham Pharmacia), and hybridized to DNA probes radiolabeled with the Prime-It II reagents as directed (Stratagene). Filters were washed twice in 2× SSC at room temperature and twice in 0.5× SSC at 65°C and then were analyzed by autoradiography.

Antisera Production. The coding sequence of mVAP33 was cloned into the bacterial expression vector pET-30a(+) as an *Eco*RI/

Abbreviations: EPSP, excitatory postsynaptic potential; ER, endoplasmic reticulum.

Data deposition: The sequence reported in this paper has been deposited in the GenBank database (accession no. AF157497).

†To whom reprint requests should be addressed. E-mail: pskehel@nimr.mrc.ac.uk.

The publication costs of this article were defrayed in part by page charge payment. This article must therefore be hereby marked "*advertisement*" in accordance with 18 U.S.C. §1734 solely to indicate this fact.

*Not*I fragment generated by a *Pfu*-based PCR with the mutagenic primer 5′-CGAATTCACCATGGCTAGCCACGAACA-3′, and the T7 primer on a cDNA clone in pcDNA1 (CLONTECH). The His_6-tagged recombinant protein was expressed in *Escherichia coli* BL21-DE3 and purified by Ni-nitrilotriacetic acid (NTA)-agarose affinity chromatography (Qiagen, Chatsworth, CA). Rabbit antisera were prepared by Murex Bioservices, Dartford, U.K.

Protein Fractionation and Western Blot Analysis. Two brains from adult male mice were homogenized with a dounce Teflon/glass homogenizer in 20 ml of ice-cold 20 mM Hepes, pH7.4/320 mM sucrose/Complete protease inhibitors (Roche Molecular Biochemicals). The homogenate was then centrifuged at $1800 \times g$ for 10 min at 4°C in a JA-20 Beckman rotor. The supernatant was removed, leaving a pellet, P1, and centrifuged again under the same conditions to remove traces of P1. P2 and S2 were then produced by similar centrifugation but at $48{,}000 \times g$ for 30 min. P2 was re-suspended in 5 ml of cold 20 mM Hepes, pH 7.4/100 mM KCl. Aliquots (1 ml) were taken, and Triton X-100 was added to 1% (vol/vol). After incubation at 37°C or 4°C for 1h. the samples were centrifuged at $356{,}000 \times g$ in a TL100.2 at 4°C for 30 min. to generate P2–Triton X-100 and S2–Triton X-100.

Triton X-114 extracts were produced from P2 by using 1.5% detergent as described by Bordier (23).

Equivalent amounts of extract were analyzed by Western blotting. mVAP33 and syntaxin (AutogenBioclear ABB36)-specific antisera were used at dilutions of 1:2000 and 1:5000, respectively. Bound antibody was detected by using horseradish peroxidase-conjugated donkey anti-rabbit or anti-mouse serum (Jackson ImmunoResearch) and enhanced chemiluminescence [ECL (Amersham)]. Membranes were stripped with 100 mM glycine, pH 2.6.

For competition experiments, 4 μl of sera was incubated with 20 μl of 4-mg/ml His_6-tagged recombinant protein in 500 μl of blocking buffer for 30 min at room temperature. After the addition of 20 μl of Ni-NTA-agarose (Qiagen), the reaction was incubated for a further 60 min with rotation at room temperature. Agarose and bound material were removed by centrifugation.

Indirect Immunofluorescent Analysis. Mixed cultures were prepared from P2 Wistar rats essentially as previously described (24), plated on poly-L-lysine-coated glass coverslips, and cultured for 7 days. Cells were then fixed with 0.3% (vol/vol) glutaraldehyde (Sigma) in PBS, for 20 min. at room temperature. Remaining reactive groups were quenched three times for 5 min per time with freshly prepared 1% (wt/vol) sodium borohydride in PBS and then washed in PBS (4 times for 5 min per wash). Cells were then permeabilized for 30 min with 0.1% (wt/vol) Saponin (Sigma) in PBS and then washed in PBS as before. Before incubation with antisera, nonspecific protein binding was blocked by a 60-min incubation at room temperature or incubation overnight at 4°C with a solution of 10% (vol/vol) FCS/0.05% (vol/vol) NP-40 in PBS. Antisera was diluted and applied in the same blocking solution for 60 min at room temperature or overnight at 4°C and then washed (4 times at 5 min per time) in 0.05% (vol/vol) NP-40/PBS. Bound antibody was detected with appropriate secondary antisera coupled to Cy2, Cy3, or Cy5 (Jackson ImmunoResearch). Samples were analyzed on a Zeiss Axiophot or a Leica TCSNT confocal microscope.

Antisera used were VAMP/synaptobrevin (ABBV35; Autogenbioclear, Whiltshire U.K.) and Calnexin (SPA-865; StressGen Biotechnologies, Victoria, Canada).

Electron-Microscopic Immunolabeling of Dissociated Cell Cultures. Dissociated hippocampal cells were grown for 8 days on small pieces of Melinex (L 4103, Agar Scientific, Ltd., U.K.). Preparations were fixed in 3% paraformaldehyde/0.3% gluteraldehyde in PBS for 20 min. After subsequent rinsing in PBS, preparations were incubated for 30 min in 1% glycine/PBS to quench residual aldehydes, and permeabilized in 0.1% saponin (S-2149; Sigma)/PBS for 15 min. The cells were then incubated for 2 h with a rabbit polyclonal antiserum directed against mVAP33 diluted 1:1000 in incubation buffer (IB) containing PBS/1% BSA/10% normal goat serum. After rinsing and renewed incubation in 0.1% saponin (15 min), preparations were incubated for 2 h with a secondary goat anti-rabbit IgG antibody conjugated to 1.0-nm gold particles (GAR1; BB International, Cardiff, U.K.; 1:80 in IB). After rinsing in PBS (5 times for 15 min per rinse) gold particles were enlarged with a silver enhancement solution (SEKL15; BB International). For this, the preparations were washed in distilled water (twice for 5 min each) and incubated for 6 min in silver enhancement solution in the dark at room temperature. Preparations were then washed (twice for 5 min each time in distilled water; twice for 10 min each time in PBS) and postfixed in 0.5% OsO_4/PBS for 6 min at room temperature. After subsequent rinsing in PBS, preparations were dehydrated in a graded series of acetone solutions before embedding in Araldite (R 1030; Agar Scientific Ltd.). The resin was polymerized in embedding moulds at 60°C overnight. Ultrathin sections (75 nm) were cut with a Reichert Ultracut and collected on pioloform-coated single-slot nickel grids. Sections were contrasted with aqueous 1.5% uranyl acetate and Reynold's lead citrate before examination in a JEOL JEM-100CX transmission electron microscope.

Electron-Microscopic Immunolabeling of Organotypic Hippocampal Tissue Slices. The method used for electron-microscopic immunolabeling was a modified version of that described by Stirling and Graff (25). Hippocampal tissue slices (11 wk old) were fixed in 3% paraformaldehyde/0.3% gluteraldhehyde in PBS for 20 min. After rinsing in PBS (twice for 15 min each) preparations were postfixed in 0.5% OsO_4, washed, dehydrated, embedded, and cut as described above. The ultrathin sections were then etched in 2% sodium *m*-periodate (S-1878; Sigma) for 25 min. After thorough rinsing in distilled water, preparations were incubated in 1% glycine/PBS (30 min), rinsed briefly in PBS, and heated in small dishes for 10 min in phosphate-citrate buffer (0.1 M; pH 6.0) at 95°C in a small oven to unmask the epitopes. Preparations were allowed to cool for 15 min, rinsed in PBS, and preincubated in IB for 30 min at room temperature. Incubation with the primary antibody was at a dilution of 1:5000 in IB overnight at 4°C. After thorough washing in PBS and preincubation in IB (30 min), preparations were incubated for 4 h with a secondary goat anti-rabbit IgG antibody conjugated to 10-nm gold particles (Sigma G-7402, 1:80 in IB). After final washing in PBS (three times for 5 min each), the preparations were postfixed in 0.1% glutaraldehyde, rinsed in distilled water (5 min), contrasted in uranyl acetate and lead citrate, and examined as described above.

Results

Cloning and Structure of mVAP33. Comparison of the ApVAP33 cDNA to the National Center for Biotechnology Information database by using a BLAST search identified a human expressed sequence tag that showed significant homology to the 5′ portion of the *Aplysia* cDNA. This sequence was used to design degenerate oligonucleotides for a PCR generating a DNA probe from mouse brain cDNA. This DNA fragment was then used to screen a mouse brain cDNA library by hybridization. Three clones were identified, and the full sequence of the largest insert was submitted to the database (accession no. AF157497). The 1.6-kilobase cDNA contains a long ORF encoding 242 amino acids of predicted molecular mass 27.3 kDa and pI 8.79. Although there are two possible ATG initiation codons, only the down-

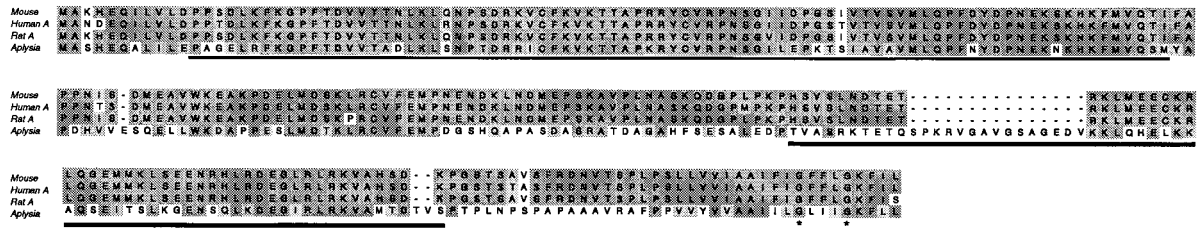

Fig. 1. Comparison of deduced VAP33 protein sequences from mouse, human, rat, and *Aplysia*. The regions of the major sperm protein homology and the predicted coiled-coil domains are indicated by thin and thick underscores, respectively. Identical and similar residues are shaded. Asterisks mark the positions of two conserved glycines that may function in coiled-coil interactions between transmembrane domains. mVAP33 GenBank accession no. AF157497.

stream sequence contains a Kozak consensus sequence (26). The predicted polypeptide is extensively homologous to the *Aplysia* protein and the human and rat sequences that were recently identified (refs. 20 and 21; Fig. 1).

The overall structures of the proteins are similar and have three obvious domains: a 100-aa domain in the N-terminal half of the protein with significant homology to the major sperm protein of *Ascaris lumbricoides*; a central domain which is potentially a coiled coil as predicted by the COILS algorithm, and a C-terminal hydrophobic domain that may anchor the protein to membranes.

In nematodes the major sperm protein assumes the function of actin in the motile spermatozoa (27) and aggregates into membrane-associated filaments by a process that is thought to underlie amoeba motility (28). The crystal structure of the major sperm protein has been solved, and residues critical for homophylic interaction have been identified by mutagenesis (29, 30). These critical residues are poorly conserved in the VAP33 peptide motif.

The primary structures of the predicted coiled-coil domains of the VAP33 proteins are less well conserved. However, human VAP33 interacts with synaptobrevin *in vitro* (21), and, similarly, the COOH-terminal 144 amino acids of mVAP33 interact with mouse VAMP/synaptobrevin in a two-hybrid assay (data not shown), indicating that the tertiary structure is conserved.

The hydrophobic C termini of the VAP33 proteins from *Aplysia californica* and mammals are highly conserved. A GXXXG motif is present in all of the VAP33 proteins. This motif has been identified in a number of transmembrane domains, where it is suggested to be required for helix–helix interactions within the membrane bilayer (31). The boundaries of the mVAP33 transmembrane domain predicted from the primary structure are ambiguous. The longest uninterrupted stretch of hydrophobic residues is 18 amino acids from L221 to G238. However, K240 precedes three additional highly hydrophobic residues. Typically transmembrane domains are between 17 and 23 residues in length. It has been demonstrated that 17-aa transmembrane domains are sufficient to retain membrane proteins in the Golgi (32).

Expression of mVAP33. By Northern blot analysis, we found mVAP33 to be expressed in all mouse tissues examined (Fig. 2). This is in contrast to *A. californica*, in which gene expression was detected primarily in the central nervous system (18).

Antisera were raised in rabbits to bacterially expressed mVAP33. A major immunoreactive protein of 33 kDa was identified by immunoblot analysis of mouse brain homogenates (Fig. 3*A*). As is the case for ApVAP33, the apparent mobility is less than that predicted from the primary structure. The specificity of this immunoreactivity was demonstrated by competition with recombinant antigen (Fig. 3*B*). mVAP33 was purified with membrane fractions from brain homogenate and was solubilized by 1% (vol/vol) Triton X-100 at 37°C (33). This extraction, however, was only partial, leaving the majority of mVAP33 in the particulate fraction. This is in contrast to the plasmallema C-terminally anchored membrane protein syntaxin, which is almost entirely extracted into the soluble phase under the same conditions [Fig. 3*A ii*]. These results suggest that mVAP33 also interacts with the cytoskeleton, possibly via the major sperm protein-homologous domain, because this protein forms cytoskeletal-like filaments (28). When solublized with Triton X-114, mVAP33 partitions entirely in the detergent phase. Notably, after Triton X-114 extraction mVAP33 appears to form an SDS-stable complex of 66 kDa. This may be the result of a homotypic interaction between hydrophobic C termini, as suggested by Nishimura *et al.* (20), perhaps involving the conserved GXXXG motif.

The similarity of the biochemical characteristics of ApVAP33 and mVAP33 and the primary structure homology of the two proteins indicate that mVAP33 is also a C-terminally anchored integral membrane protein.

Cellular Distribution of mVAP33. Indirect immunofluorescence microscopy was used to analyze the cellular distribution of mVAP33 in primary cultures from rat neocortex (Fig. 4). Both neurons and glia express mVAP33 immunoreactivity. In glia, the immunoreactivity accumulates in the perinuclear area and extends throughout the cytoplasm in a diffuse reticular pattern;

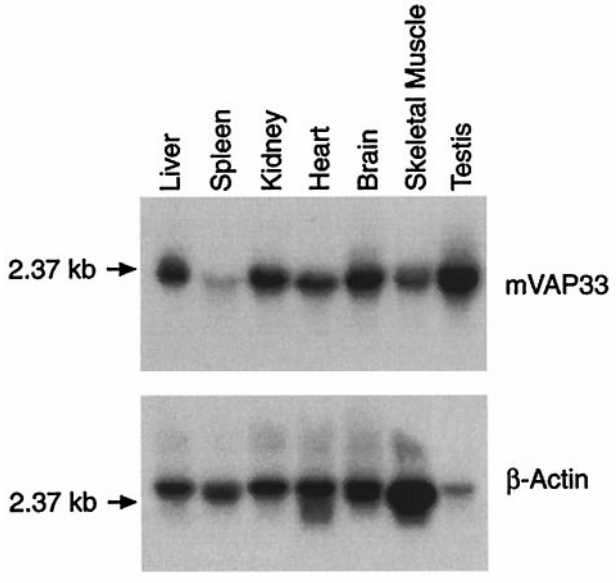

Fig. 2. Tissue distribution of mVAP33 mRNA expression. Total RNA from the tissues indicated was analyzed by Northern blot hybridization. Parallel blots were hybridized with radiolabeled mVAP33 or mouse β-actin cDNAs. mVAP33 transcripts of ≈2 kilobases are detectable in all tissues analyzed.

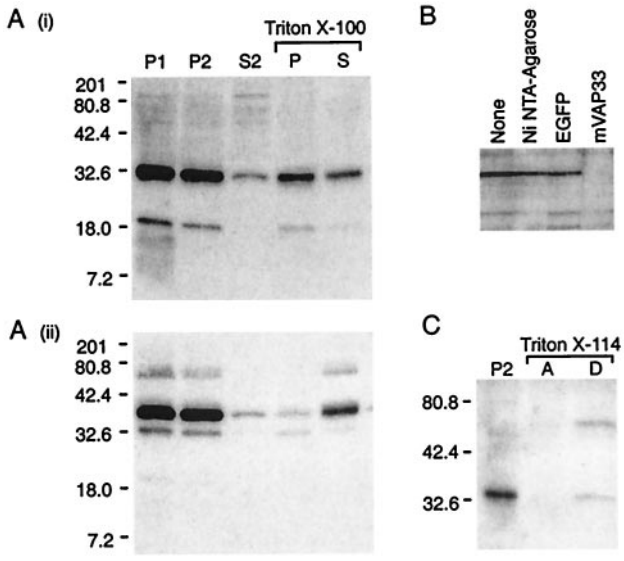

Fig. 3. (*A*) Western blot analysis of fractionated mouse brain homogenate with mVAP33-specific polyclonal antiserum. (*i*) The major immunoreactive signal of ≈33 kDa is enriched in the pelleted fractions, but it is only partially extracted into the soluble fraction by 1% (vol/vol) Triton X-100. The cofractionating 19-kDa signal may be the result of proteolysis. (*ii*) In contrast, the t-SNARE syntaxin, although present in P1 and P2, is almost completely extracted by Triton X-100. The lower-molecular-weight signal is the result of incomplete stripping of the mVAP33 antisera. Molecular markers are Kaleidoscope Prestained Standards (Bio-Rad). (*B*) The 33-kDa immunoreactivity is specific for mVAP33. The antisera were preincubated with Ni-NTA-agarose with or without recombinant protein. Ni-NTA-agarose, or Ni-NTA-agarose and His_6-tagged recombinant green fluorescent protein (EGFP) have no affect, whereas His_6-tagged recombinant mVAP33 specifically depletes the 33-kDa signal. (*C*) mVAP33 is an integral membrane protein. P2 was extracted with 1.5% Triton X-114 and separated into aqueous (A) and detergent (D) phases at 37°C. The 33-kDa immunoreactivity partitions into the detergent phase, indicating that, like the molluscan protein, mVAP33 is an integral membrane protein. After Triton X-114 extraction, mVAP33 appears to form an SDS-stable oligomer of approximately 66 kDa.

neurons also show a perinuclear accumulation. In addition, the signal extends throughout most of the cell processes. This distribution is distinct from that of VAMP/synaptobrevin (Fig. 4). Processes of all calibers appear to be labeled. A similar distribution is seen for calnexin (Fig. 4; ref. 34). More detailed inspection of neuronal processes reveals mVAP33 immunoreactivity in a punctate distribution that may reflect larger complexes or aggregates of protein. These results suggest that mVAP33 is present in the endoplasmic reticulum (ER) membrane. This is consistent with the relatively short hydrophobic C-terminal domain of the protein because transmembrane domains of 17 amino acids have been shown to retain membrane proteins in the ER/Golgi (32). The yeast protein SCS2 shows extensive identity with mVAP33 and has been localized to the ER (22). This report also analyzed the topology of the protein in relation to the ER membrane, demonstrating that the amino terminus of the protein is cytoplasmic. ApVAP33 was originally identified by its ability to interact with VAMP/synaptobrevin in a yeast two-hybrid assay, and the mammalian protein has a similar activity (21; data not shown). However, unlike VAMP/synaptobrevin, mVAP33 is not enriched at synaptic sites (Fig. 4). There is no indication of immunoreactivity at the plasma membrane. Moreover, although mVAP33 often appears microscopically as aggregates, these structures do not colocalize with VAMP/synaptobrevin (Fig. 4). This suggests that mVAP33 is retained in the ER and that any interaction with VAMP/synaptobrevin is transient and before this protein's accumulation on mature synaptic vesicles.

Ultrastructural Analysis of mVAP33. Immunogold electron microscopic analysis of organotypic hippocampal slice cultures and dissociated cortical cell cultures identified mVAP33-specific immunoreactivity associated with three types of structures. First, in organotypic cultures, there was a low level of immunoreactivity that was mainly associated with microtubules (Fig. 5*A*). There were multiple gold particles often clustered on a single microtube (Fig. 5 *B* and *C*). Second, multiple sites of immunoreactivity were also seen associated with the membranes of vesicular structures (Fig. 5 *D* and *E*). Third, occasionally the

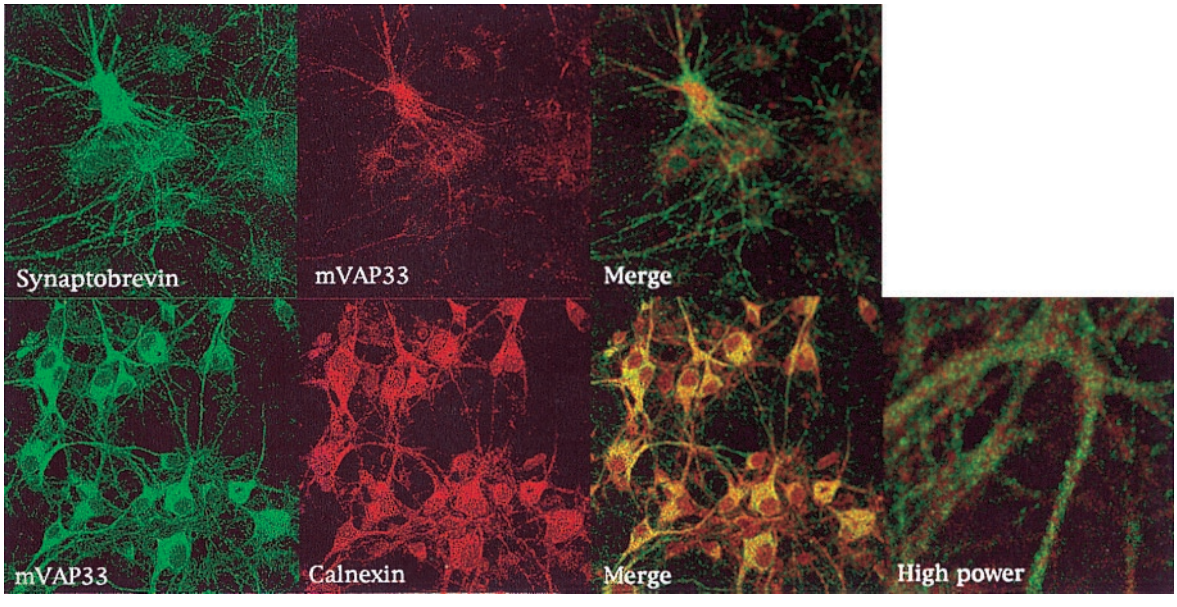

Fig. 4. Indirect immunofluorescence analysis of cultured cortical cells. Cortical cells were prepared from P2 Wistar rats and maintained in culture for 7 days before fixation and analysis. Cultures were stained with the specific antisera indicated. mVAP33 does not colocalize with VAMP/synaptobrevin at synaptic terminals, but has a reticular dstribution in glia and neurons. There is extensive colocalization of mVAP33 and the ER protein calnexin. At higher power, mVAP33 immunoreactivity shows a punctate distribution distinct from that of calnexin.

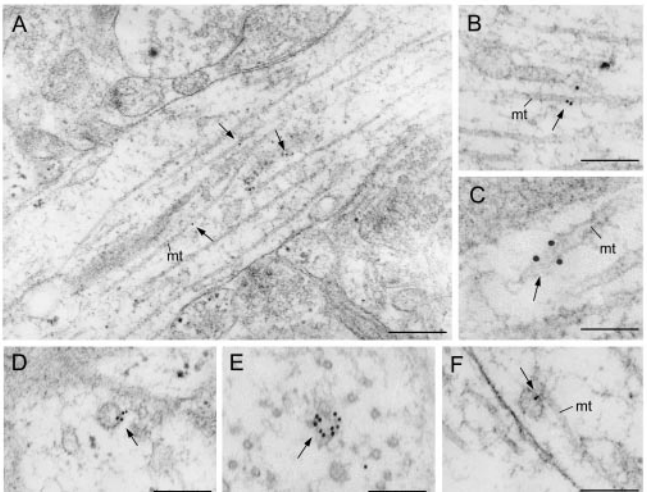

Fig. 5. Immunogold labeling of hippocampal organotypic cultures for mVAP33. Immunoreactivity was mainly associated with microtubules (*A*), where it was often clustered (*B* and *C*). Clustered labeling was also associated with the membranes of vesicular structures (*D* and *E*). Gold particles were also occasionally seen between a vesicle and a microtubule (*F*). There was no detectable signal associated with synaptic vesicles. (Bars: *A*, 300 nm; *B* and *D*, 200 nm; *C*, 100 nm; *E*, 150 nm; and *F*, 80 nm.)

point of association between a vesicle and a microtubule was also labeled (Fig. 5*F*). There was no detectable signal associated with synaptic vesicles or the plasma membrane.

We also analyzed cortical neurons in dissociated culture. Here the level of immunoreactivity was generally higher, consistent with immunofluorescent analysis (Fig. 4 and data not shown). The neuronal processes contained large numbers of heterogeneously sized membrane-bound structures (Fig. 6 *A–C*). mVAP33 was frequently associated with the surface of these vesicles, often at electron dense structures (Fig. 6*D*). In addition

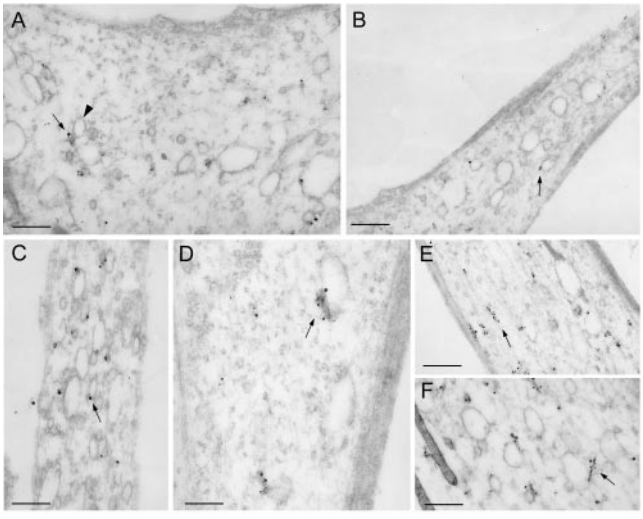

Fig. 6. Immunogold labeling of mVAP33 in cultured cortical cells. Neuronal processes contained large numbers of heterogeneously sized membrane-bound structures (*A*, *B*, and *C*, arrows) that were frequently labeled. Labeling often coincided at electron-dense structures (*D*, arrow). Larger extended aggregates of mVAP33 immunoreactivity were occasionally detected in short filamentous structures that were frequently localized with membrane structures (*E* and *F*, arrows). (Bars: *A* and *C*, 400 nm; *B*, 650 nm; *D*, 250 nm; *E*, 850 nm, and *F*, 550 nm.)

to this discrete membrane-associated signal, larger extended aggregates of mVAP33 immunoreactivity were also detected in short filamentous structures that were also frequently localized with membranes (Fig. 6 *E* and *F*).

Discussion

Since the initial isolation of *Aplysia* VAP33, homologous proteins have been described from humans, rats, yeasts, and now mice. In addition there are similar sequences in the databases for *Caenorhabditis elegans* and *Arabidopsis*. In contrast to the restricted expression pattern seen in *A. californica* (18), the VAP33 homologues are more ubiquitously expressed, which suggests a general rather than a neuron-specific function.

Ultrastructural and biochemical analysis of mVAP33 indicates several features of the molecule that can be related to its primary structure. mVAP33 purifies as an integral membrane protein that is present on intracellular membranes in a reticular distribution. In addition to its membrane localization, mVAP33 also seems to associate with microtubules, and can form larger aggregates that may be associated with cytoskeletal elements. The major sperm protein forms a cytoskeletal structure in the amoeboid spermatazoa (28), and although the residues critical for major sperm protein oligomerization are not well conserved in the homologous N-terminal domain of mVAP33, this region could contribute to this aggregated distribution. Whereas coiled coils are a common structural motif found in some microtubule-binding proteins (35, 36), mVAP33 contains no primary structural features with homology to known microtubule-binding motifs. Another type II integral membrane protein, p63, was recently shown to interact directly with microtubules (37).

Microinjection of ApVAP33-specific antisera into the presynaptic cell of a sensorimotor-cell coculture leads to a reduction in the evoked EPSP when measured several hours later (18). The gross structural similarity between syntaxin and ApVAP33 originally suggested that both molecules might have similar functions in mediating synaptic-vesicle interaction with the presynaptic plasma membrane. This is unlikely to be the case for mVAP33. Although there may be additional members of a VAP33 gene family, our immunocytochemical and ultrastructural analysis suggests that mVAP33 associates mainly with ER membranes and microtubules, consistent with a function in intracellular transport, because vesicle and organelle trafficking requires interaction with the microtubule network (1). Thus, the simplest idea for the function of mVAP33 might be that it has a role in trafficking or chaperoning vesicular components such as VAMP/synaptobrevin through the ER and on to the synaptic terminals. A similar function has been suggested for another VAMP/synaptobrevin-binding protein BAP31 (12). Based on this view, intracellular injection of mVAP33 antisera could reduce evoked EPSP by inhibiting vesicular transport, leading to a depletion of limiting components at the synaptic terminal. In this case, mVAP33 would have a general function in intracellular transport. Unlike VAMP/synaptobrevin, mVAP33 does not accumulate at synaptic sites. Any functional interaction that may exist between the two molecules, therefore, is probably within the ER. VAMP/synaptobrevin is inserted into the ER membrane post-translationally by a saturable ATP-dependent mechanism (38). It is possible that mVAP33 might function in the process directly or act as a chaperonelike protein, facilitating VAMP/synaptobrevin's passage through the ER system. In either case, inhibiting the function of mVAP33 by antibody injection could lead to reductions in the levels of VAMP/synaptobrevin on synaptic vesicles, resulting in a reduction in the efficiency of exocytosis. This would be consistent with mini-EPSP analysis of the inhibited *Aplysia* cocultures, which showed no overall reduction in amplitude or frequency of spontaneous or osmotically evoked release, but a 50% decrease in electrically evoked EPSP (P.A.S., M. Giarardi, and E.R.K., unpublished work).

Another possibility is suggested by the knock-out of a VAP33 homologue, SCS2, in yeasts, that causes a perturbation of an ER-to-nucleus signaling system. Nikawa *et al*. isolated SCS2 as a high copy suppressor of an inositol auxotrophic mutation (39) and subsequently showed that deletion of the gene resulted in inositol auxotrophy (22). Notably, deletion of SCS2 did not result in a detectable secretion phenotype. This may indicate that the inhibition of evoked EPSP in the *Aplysia* coculture is a secondary consequence of disrupting a process that is distinct from synaptic-vesicle and plasma membrane fusion.

In yeasts, the inositol biosynthesis pathway shares much of the same regulatory pathway with the Unfolded Protein Response (UPR; 40). The central regulator of the yeast UPR, *IRE1*, has recently been identified in humans, indicating that a similar signaling system is present in higher eukaryotes (41). The UPR is stimulated by accumulation of immature polypeptides in the lumen of the ER, which is signaled through activation of the transmembrane kinase/nuclease Ire1p (42). It has been suggested that the UPR and inositol biosynthesis pathways are coregulated to coordinate the protein modification and chaperone capacity of the ER with its size. Kagiwada *et al.* have proposed that SCS2 may act as a transcription factor signaling a heat shock response by proteolytic activation (22). Although a possible proteolyzed derivative of mVAP33 was detected by Western blot (Fig. 3), there was no evidence for nuclear localization of mVAP33 immunoreactivity by fluorescence or electron microscopy. The phenotype of the SCS2 mutation was more pronounced at higher temperatures, and it was argued that this may reflect an involvement with the heat shock response (22). A structural homologue of VAP33 has been identified in *Arabidopsis* after its induction by osmotic shock (43). Although in this case the protein appears to be localized to the plasma membrane, it is consistent with VAP33 proteins having some function in membrane metabolism.

The structure of the ER is maintained by interactions between the ER membrane and the microtubules. Perhaps mVAP33, which faces the cytoplasm from the ER membrane, may have a signaling activity to coordinate the levels of type II membrane proteins with the size or capacity of the ER. A striking feature from the ultrastructural localization analysis of mVAP33 is its association with vesicular membranes and microtubules, frequently at a point of close juxtaposition between these structures. The hydrophobic C terminus of mVAP33 most likely mediates a direct interaction with the membrane, but the nature of the microtubule association is not clear. In this way, in addition to a possible signaling activity, mVAP33 may have a more direct function in maintaining or regulating distribution of the ER or ER-like organelles within the cell.

We thank Drs. Vincent O'Conner, Tim Bliss, Michael Stewart, and Dusan Bartsch for their help during the course of this work and the preparation of the manuscript.

1. Cole, N. B. & Lippincott-Schwartz, J. (1995) *Curr. Opin. Cell Biol.* **7,** 55–64.
2. Lee, C. & Chen, L. B. (1988) *Cell* **54,** 37–46.
3. Nichols, B. J. & Pelham, H. R. (1998) *Biochim. Biophys. Acta* **1404,** 9–31.
4. Fernandez-Chacon, R. & Sudhof, T. C. (1999) *Annu. Rev. Physiol.* **61,** 753–776.
5. Jahn, R. & Sudhof, T. C. (1994) *Annu. Rev. Neurosci.* **17,** 219–246.
6. Sollner, T., Bennett, M. K., Whiteheart, S. W., Scheller, R. H. & Rothman, J. E. (1993) *Cell* **75,** 409–418.
7. Sollner, T., Whiteheart, S. W., Brunner, M., Erdjument-Bromage, H., Geromanos, S., Tempst, P. & Rothman, J. E. (1993) *Nature (London)* **362,** 318–324.
8. Hanson, P. I., Heuser, J. E. & Jahn, R. (1997) *Curr. Opin. Neurobiol.* **7,** 310–315.
9. Ungermann, C., Sato, K. & Wickner, W. (1998) *Nature (London)* **396,** 543–548.
10. Naren, A. P., Nelson, D. J., Xie, W., Jovov, B., Pevsner, J., Bennett, M. K., Benos, D. J., Quick, M. W. & Kirk, K. L. (1997) *Nature (London)* **390,** 302–305.
11. Quick, M. W., Corey, J. L., Davidson, N. & Lester, H. A. (1997) *J. Neurosci.* **17,** 2967–2979.
12. Annaert, W. G., Becker, B., Kistner, U., Reth, M. & Jahn, R. (1997) *J. Cell Biol.* **139,** 1397–1410.
13. Bennett, M. K., Calakos, N. & Scheller, R. H. (1992) *Science* **257,** 255–259.
14. David, P., el Far, O., Martin-Mouto, N., Poupon, M. F., Takahashi, M. & Seagar, M. J. (1993) *FEBS Lett.* **326,** 135–139.
15. Hata, Y., Slaughter, C. A. & Sudhof, T. C. (1993) *Nature (London)* **366,** 347–351.
16. Leveque, C., el Far, O., Martin-Moutot, N., Sato, K., Kato, R., Takahashi, M. & Seagar, M. J. (1994) *J. Biol. Chem.* **269,** 6306–6312.
17. Linial, M., Ilouz, N. & Parnas, H. (1997) *J. Physiol.* **504,** 251–258.
18. Skehel, P. A., Martin, K. C., Kandel, E. R. & Bartsch, D. (1995) *Science* **269,** 1580–1583.
19. Betz, A., Okamoto, M., Benseler, F. & Brose, N. (1997) *J. Biol. Chem.* **272,** 2520–2526.
20. Nishimura, Y., Hayashi, M., Inada, H. & Tanaka, T. (1999) *Biochem. Biophys. Res. Commun.* **254,** 21–26.
21. Weir, M. L., Klip, A. & Trimble, W. S. (1998) *Biochem. J.* **333,** 247–251.
22. Kagiwada, S., Hosaka, K., Murata, M., Nikawa, J. & Takatsuki, A. (1998) *J. Bacteriol.* **180,** 1700–1708.
23. Bordier, C. (1981) *J. Biol. Chem.* **256,** 1604–1607.
24. Bekkers, J. M. & Stevens, C. F. (1989) *Nature (London)* **341,** 230–233.
25. Stirling, J. W. & Graff, P. S. (1995) *J. Histochem. Cytochem.* **43,** 115–123.
26. Kozak, M. (1987) *J. Mol. Biol.* **196,** 947–950.
27. Bullock, T. L., McCoy, A. J., Kent, H. M., Roberts, T. M. & Stewart, M. (1998) *Nat. Struct. Biol.* **5,** 184–189.
28. Italiano, J. E., Jr., Roberts, T. M., Stewart, M. & Fontana, C. A. (1996) *Cell* **84,** 105–114.
29. Bullock, T. L., Roberts, T. M. & Stewart, M. (1996) *J. Mol. Biol.* **263,** 284–296.
30. Smith, H. E. & Ward, S. (1998) *J. Mol. Biol.* **279,** 605–619.
31. Brosig, B. & Langosch, D. (1998) *Protein Sci.* **7,** 1052–1056.
32. Munro, S. (1995) *EMBO J.* **14,** 4695–4704.
33. Schroeder, R., London, E. & Brown, D. (1994) *Proc. Natl. Acad. Sci. USA* **91,** 12130–12134.
34. Krijnse-Locker, J., Parton, R. G., Fuller, S. D., Griffiths, G. & Dotti, C. G. (1995) *Mol. Biol. Cell* **6,** 1315–1332.
35. De Zeeuw, C. I., Hoogenraad, C. C., Goedknegt, E., Hertzberg, E., Neubauer, A., Grosveld, F. & Galjart, N. (1997) *Neuron* **19,** 1187–1199.
36. Pierre, P., Scheel, J., Rickard, J. E. & Kreis, T. E. (1992) *Cell* **70,** 887–900.
37. Klopfenstein, D. R., Kappeler, F. & Hauri, H. P. (1998) *EMBO J.* **17,** 6168–6177.
38. Kutay, U., Ahnert-Hilger, G., Hartmann, E., Wiedenmann, B. & Rapoport, T. A. (1995) *EMBO J.* **14,** 217–223.
39. Nikawa, J., Murakami, A., Esumi, E. & Hosaka, K. (1995) *J. Biochem.* **118,** 39–45.
40. Cox, J. S., Chapman, R. E. & Walter, P. (1997) *Mol. Biol. Cell* **8,** 1805–1814.
41. Tirasophon, W., Welihinda, A. A. & Kaufman, R. J. (1998) *Genes Dev.* **12,** 1812–1824.
42. Chapman, R., Sidrauski, C. & Walter, P. (1998) *Annu. Rev. Cell. Dev. Biol.* **14,** 459–485.
43. Galaud, J. P., Laval, V., Carriere, M., Barre, A., Canut, H., Rouge, P. & Pont-Lezica, R. (1997) *Biochim. Biophys. Acta* **1341,** 79–86.